"Spin Dependent Tunneling Magnetic Field Sensors for Clutter-Limited Detection"

7-24-2002

Sponsored by
Defense Advanced Research Projects Agency (DOD)
SPO

ARPA Order K475/37

Issued by U.S. Army Aviation and Missile Command Under Contract No. DAH01-02-C-R

NVE Corporation
11409 Valley View Road
Eden Prairie, MN 55344

Effective Contract Date October 17, 2001
Contract Expiration Date June 28, 2002
Principal Investigator Mark Tondra, (952) 996-1615, MarkT@nve.com

SDT Sensors for Clutter-Limited Detection

Reporting Period Entire Program: October 17th – June 28th, 2002

ABSTRACT

The objective of this Phase I SBIR project is to develop a low power magnetic field sensor for use in clutter-limited detection environments, and to evaluate concepts for self-calibration of this field sensor under particular deployment conditions. The underlying technology for the sensor development is Spin Dependent Tunneling, an advanced form of magnetoresistance. The unique aspect of SDT that is particularly attractive for this application is its intrinsically high impedance, which leads naturally to low power sensing devices. Previous sensor designs using SDT devices required about 200 mW of power to provide a magnetic field bias. A key effort in this project is to demonstrate a sensor design that does not require this electrical current-based magnetic field bias. Sensors employing a magnetic "shape-bias" have been fabricated, packaged, and successfully demonstrated. This report contains the first results from these sensors, including sensitivity and noise vs. frequency data. Also, a study of power vs. sensor resistance was performed in which the power for the magnetic transducer and low noise amplifier were added together to get a total power.

Taken together, it appears as if SDT sensors could meet all of the "Clutter-Limited Detection" sensor requirements at some point. Most are already demonstrated.

UNCLASSIFIED

Executive Summary

This is the final report for a Phase I SBIR project entitled "Spin Dependent Tunneling Magnetic Field Sensors for Clutter-Limited Detection". This report covers progress through the entire project period.

This report describes the successful demonstration of a new LOW POWER version of the Spin Dependent Tunneling (SDT) magnetic field sensor. The old versions of SDT sensors required a magnetic field bias to create ideal operating conditions. This field bias had been generated by passing electrical current through an on-chip coil. The new version replaces the current-based biasing with a "shape" biasing that requires no additional power. A small amount of wafer fabrication has continued since the Second Quarter Report was filed.

KEY RESULT The low power SDT sensors were fabricated and tested during this Phase I SBIR project. The early results are promising, particularly in the hysteresis characteristics. The sensitivity and noise are good, though not fully optimized. Their power requirements are well less than 1 mW at 5 Volts, thus meeting one of the "Clutter Limited Detection" solicitation specifications.

This report is divided into five main technical sections. The new results are in Section 3, and application concepts are in Section 5. Each section is self-contained and can be read without reading the others. They are as follows:

1. Program Goals (from Phase I Proposal)
2. Low power sensor fabrication
3. Low power sensor results: transfer curve and noise evaluation
4. Sensor + amplifier power analysis
5. CUFG application possibilities

In addition to these technical sections, there are several appendices with supporting information:

Appendix A. Program Schedule
Appendix B. Budget
Appendix C. Comparative Technology Study

1. Program Goals

In review, the program objectives as stated in the solicitation are below:

- *(A) Modest size: individual receivers should have maximum dimension of 10 cm or less;*
- *(B) Low power: less than milliwatt of average power per receiver;*

- *(C) Broad band: 10 Hertz to 2000 Hertz (although higher frequencies – up to 30 KHz are of interest);*
- *(D) High sensitivity: for B field, noise equivalent performance less than 5 picoTesla/root Hz in the 10 Hz to 300 Hz frequency range, noise equivalent performance less than 0.5 picoTesla/root Hz in the 300 Hz to 2000 Hz frequency range; noise equivalent performance of electric-field sensors should be below the clutter background.*
- *(E) High dynamic range: receiver linearity and dynamic range (not digitizer) - capable of a linear output over a range of 80 dB;*
- *(F) Robust outdoor performance: insensitive to likely levels of insitu vibrations (wind noise, seismic noise) or to significant changes in ambient temperature (-20 degrees to 50 degrees C) and humidity variations (5 -100% relative), and insensitive to shock (less than 100 g's).*

The characteristics presented above do not include the power source (e.g. batteries), digitizing electronics, local processing or communications.

In order to meet some of these goals, program objectives were stated in NVE's proposal as:

The overall goal of this Phase I SBIR effort is to:

Develop a concept for using Spin Dependent Tunneling magnetic field sensors in a self-calibrating self-orienting long-baseline fielded gradiometer.

This will require effort in the following areas
1) Low Power SDT sensor fabrication and testing
2) Comparative technology study
3) Fielded system conceptualization

2. Low Power SDT Sensors Fabrication

This section is mostly a repeat from the first quarterly report. It is include here for those who want a detailed explanation of SDT sensor design and fabrication. If this is not the case, one is best off skipping to the new results shown in Section 3.

An SDT device consists of two magnetic thin films separated by an ultra-thin insulating tunneling barrier. By a quantum mechanical process called "tunneling" electrons can pass through the insulator from one magnetic film to the other. The "tunneling resistance" is dependent on the relative orientation of the magnetization in the two magnetic films. In a SDT magnetic sensor, the magnetization of one of the magnetic films is held fixed or "pinned" while the other is allowed to rotate in response to an external field. In this way, a device is created whose resistance is sensitive to an applied field. The sign of the effect is such that the resistance is least when the magnetizations of the two magnetic layers are parallel and greatest when they are anti-parallel. The field-varying portion of the tunneling resistance typically represents an increase from the nominal (magnetizations parallel) resistance on the order of 30-50%

(for the types of films used at NVE) and is proportional to the sine of the angle between the magnetizations of the two magnetic films as shown in Fig. 3.

The standard layer structure of materials used to make SDT devices is also shown in Fig. 3. In these structures, the bottom ferromagnetic layer (NiFeCo) is free to rotate in response to the applied film, while the top synthetic ferromagnetic layer (CoFe / Ru / CoFe) is magnetically pinned in place by the adjacent antiferromagnetic layer (CrPtMn). The tunneling barrier is made of Al_2O_3.

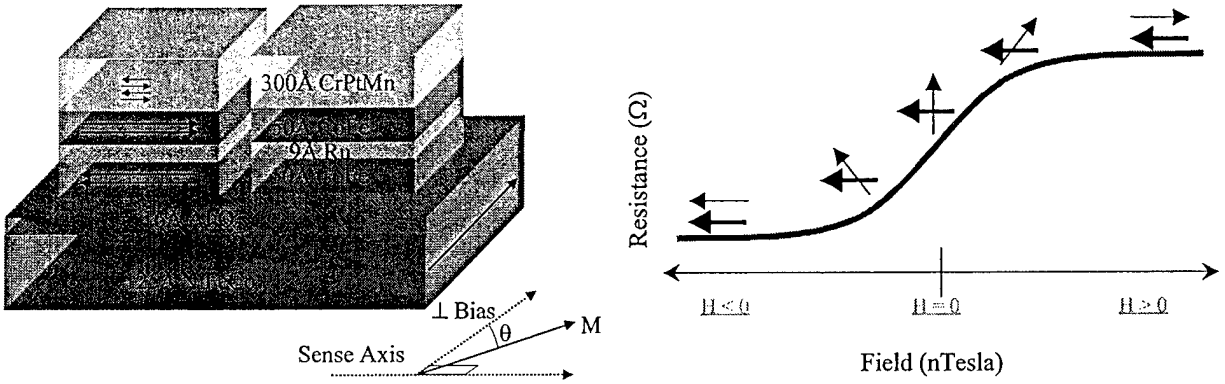

Figure 3. At left is a cross section schematic of NVE's standard layered structure of a SDT device with a pinned (top) ferromagnetic film. At right is a plot depicting the change in resistance as the soft layer magnetization rotates with respect to the hard layer magnetization. The plot shows how the rotation takes place due to an external applied field along the sense axis. Without the perpendicular bias, the free layer magnetization would "flip" suddenly rather than rotate smoothly.

The tunnel junction films are patterned in a series of deposition, lithography and etch steps in a process similar to that used to manufacture integrated circuits. The result is shown graphically in Fig. 4. Generally contact is made to the top magnetic layer only, and a single tunnel junction "element" actually consists of two tunnel junctions, which share a common bottom magnetic layer. Devices with sizes ranging from $5\mu m^2$ to 1,000,000 μm^2 have been fabricated at NVE. On NVE's current experimental sensor chips, several tunnel junction elements are wired in series for increased sensitivity.

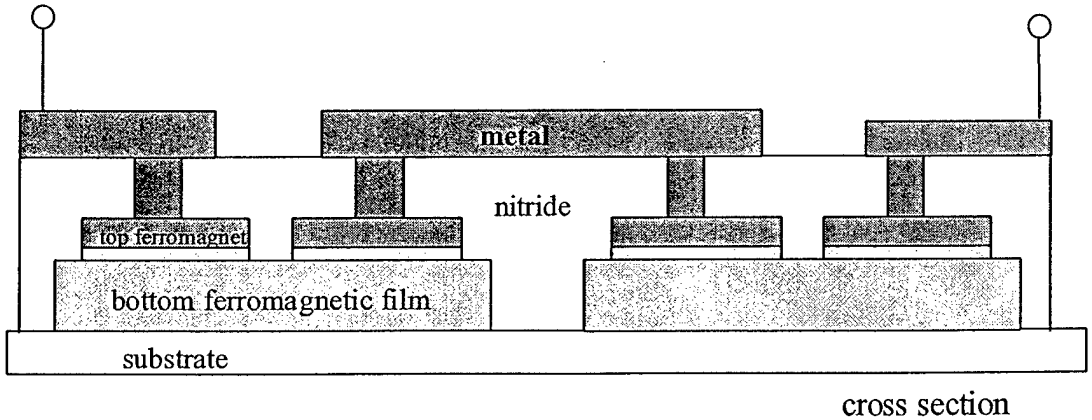

Figure 4. Schematic view of a series of patterned SDT devices interconnected with a patterned Al trace.

NVE's most recently developed SDT prototype sensor contains a Wheatstone bridge configuration of sensors and uses magnetic shielding over two of the legs of the bridge. The shields over opposite legs cause the magnetoresistance change of the unshielded two to be measured as a voltage output on the otherwise matched bridge. A second function of the shields is to produce a flux concentrating effect. The thick magnetic films are also known as flux concentrators and can be used to advantage if the unshielded elements are placed in a small gap between the two halves. As shown in Fig. 5, the flux concentrators increase the field seen by the elements in the gap by a factor approximately equal to the length divided by the gap width.

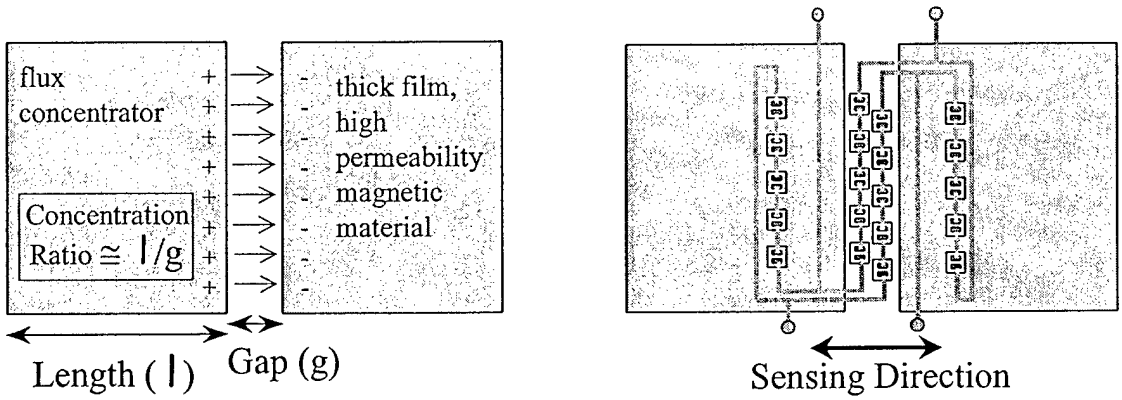

Figure 5: Bridge sensor with flux concentrators.

The sensor design also includes two sets of on-chip coils. As pictured in Fig. 6, one coil produces a field which is parallel to the sensing direction and is used to provide a zeroing field for the sensor in order to offset background fields such as the earth's field. The second coil provides a field in the direction perpendicular to the sensing direction and is used to orthogonally bias the sensor as described earlier. *It is the need to eliminate the 200 mW of power consumed by this coil that is driving the present effort.*

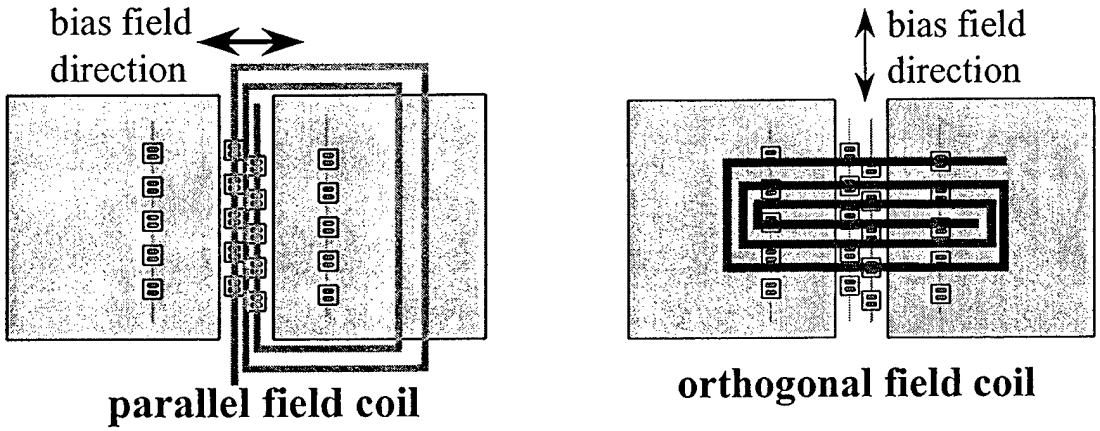

Figure 6: Drawing of the two on-chip coils for NVE's SDT sensor.

Orthogonal Field Biasing

Typical resistive response as a function of the applied field is shown in Fig. 7. The large change in resistance occurs when the free layer magnetization changes direction from parallel to the pinned layer to anti-parallel and vice versa. The large hysteresis seen in Fig. 7 makes this response unsuitable for a field sensor. In order to achieve a low-hysteresis linear response, the device is biased with a magnetic field applied perpendicular to the sensitive axis. The beneficial effect of this bias field is shown in Fig. 8. As the orthogonal bias is increased to its optimum value (just above the coercivity of the free layer), the hysteresis is reduced and a more stable and reproducible resistance-versus-field curve is obtained.

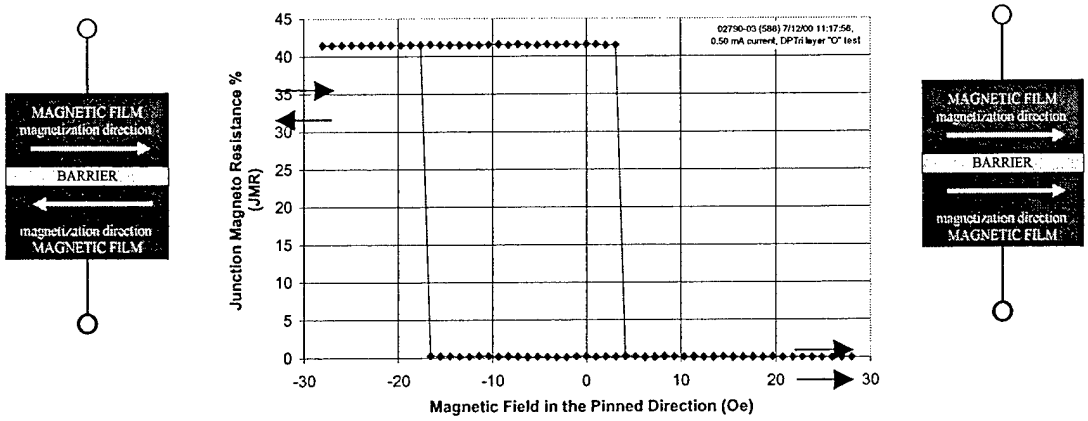

Figure 7: Magnetoresistive data from a SDT device. The asymmetry of the switching fields about zero field is due to magnetic coupling between the two magnetic layers across the insulating barrier. The applied field is parallel to the pinned direction. Junction magnetoresistance (JMR) is defined as the maximum change in resistance divided by the resistance of the state in which both magnetic layers are parallel (low resistance state).

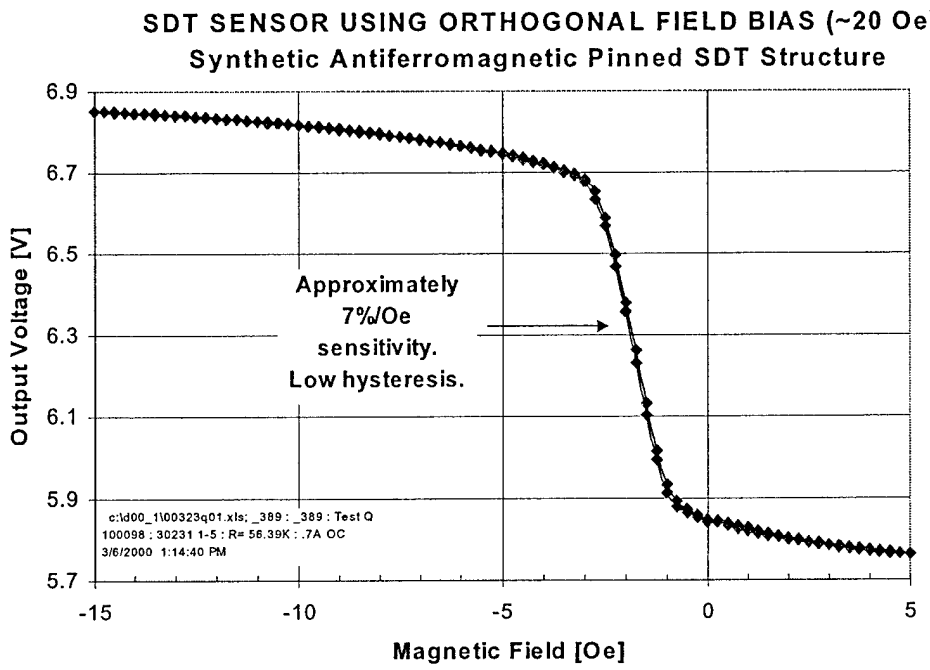

Figure 8: The effect on the output voltage vs. sensing-axis field of an SDT sensor when subjected to an orthogonal magnetic field bias. A constant current is applied to power the sensor. As the applied orthogonal field strength slightly exceeds the coercive field, the hysteresis will vanish. As the field strength is increased beyond this, the sensitivity of the sensor will decrease further.

Two views of the new shape-biased SDT devices are shown below in Figs. 9 and 10. The main difference is that the tunnel junctions are long and narrow, such that the long direction is perpendicular to the sensitive direction. Another difference is that the etching of the lower electrode is somewhat longer.

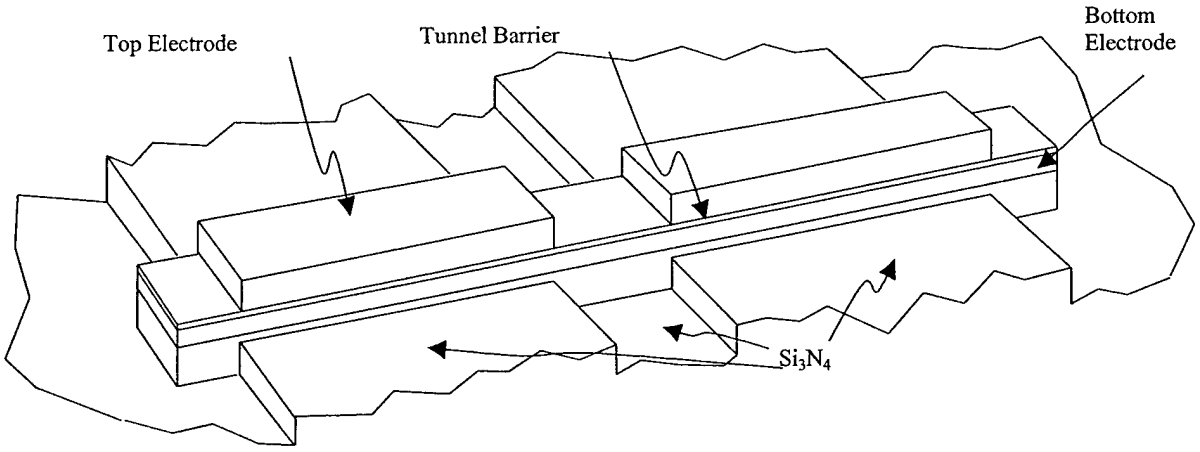

Figure 9. This structure is the result of using photolithography masks where the top and bottom electrode shapes overlap. The top electrode mask for this is two parallel stripes running into the page. The bottom electrode mask is a single stripe running across the page. Tunnel junctions exist where the two masks overlap, and connections between the two junctions exist where there was a bottom mask but no top mask.

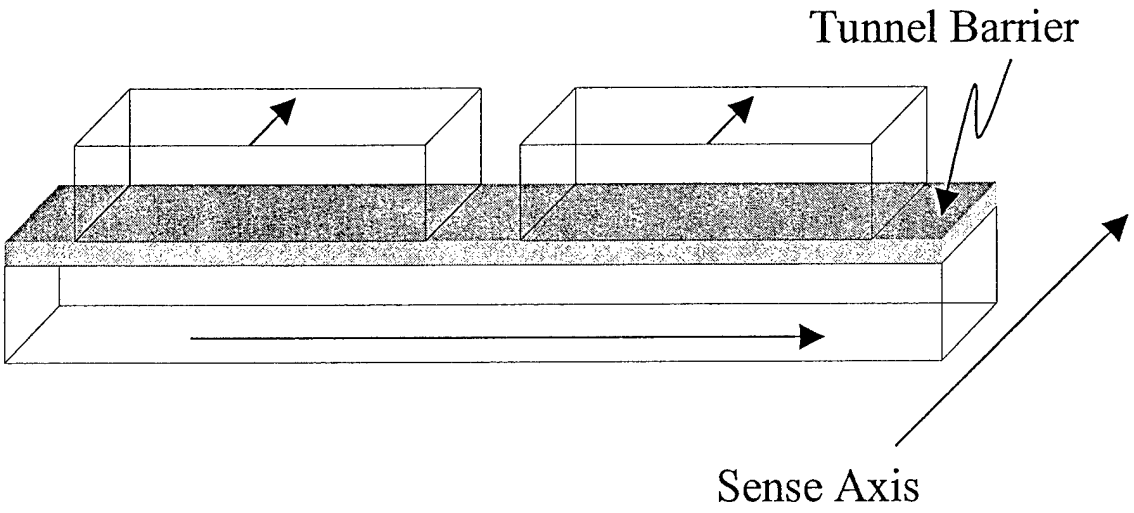

Figure 10. A view of the actual junction components in the structure shown above. The advantage of etching this way is that the top and bottom electrodes can have coincident edges, saving space and making narrower junctions possible.

The structures above are the result of two cuts. Note that the interconnecting Al metal layer is not shown here. The first cut is done with a mask over the two parallel structures running from front to back in the diagram. The second cut is done with a mask over the long narrow structure running from left to right. The first cut removes material down to the tunnel barrier. The second cut removes material all the way through the tunnel junction structure (top electrode, barrier, and bottom electrode) and into the underlying Si_3N_4 . Those areas that are left exposed for both etches have material removed even more deeply in the Si_3N_4 . The result is a long narrow bottom electrode with two narrow top electrodes sitting on it. The current flow through such a structure is in through the top electrode on one side, down through that tunnel barrier into the bottom electrode, along the bottom electrode to the other tunnel barrier, and up through the barrier into the other top electrode.

Early results from some of these devices made in earlier projects are promising. An example is shown in Fig. 11. The patterning was okay for this device, but some annealing details need continued effort to really optimize this sensor output. An improved transfer curve was achieved in GMR devices by making the bottom sensing film a NiFeCo / Ru / NiFeCo sandwich rather than a simple NiFeCo layer. The magnetoresistive results of GMR "spin valve" structures made with this type of free layer are shown in Figs. 12 and 13. This Phase I project has successfully incorporated this free layer into a tunnel junction (NEW RESULTS IN Section 3).

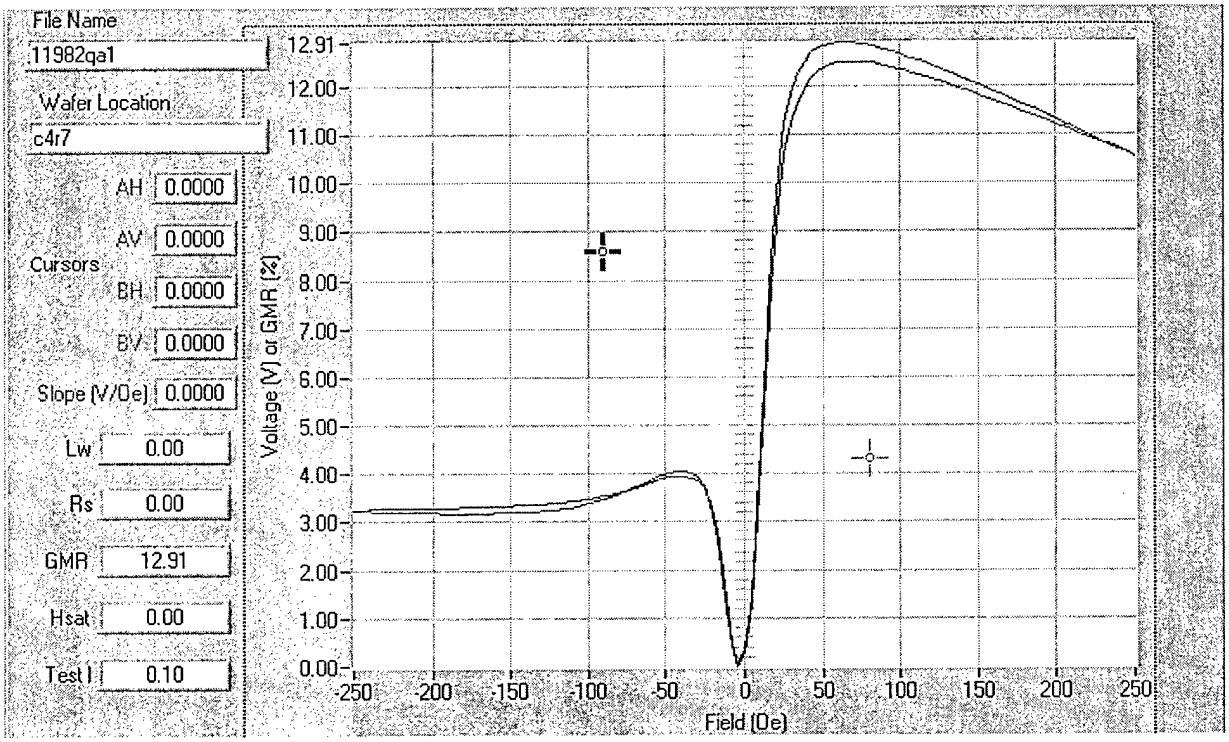

Figure 11. Two terminal resistance data from shape biased SDT sensor bridges. The sensors do not yet have flux concentrators, so they do not behave as a sensor, with a field-dependent bridge offset. Flux concentrators will also compress the effective field scale, so that the sensor saturates at about 5 Oe rather than 50 Oe.

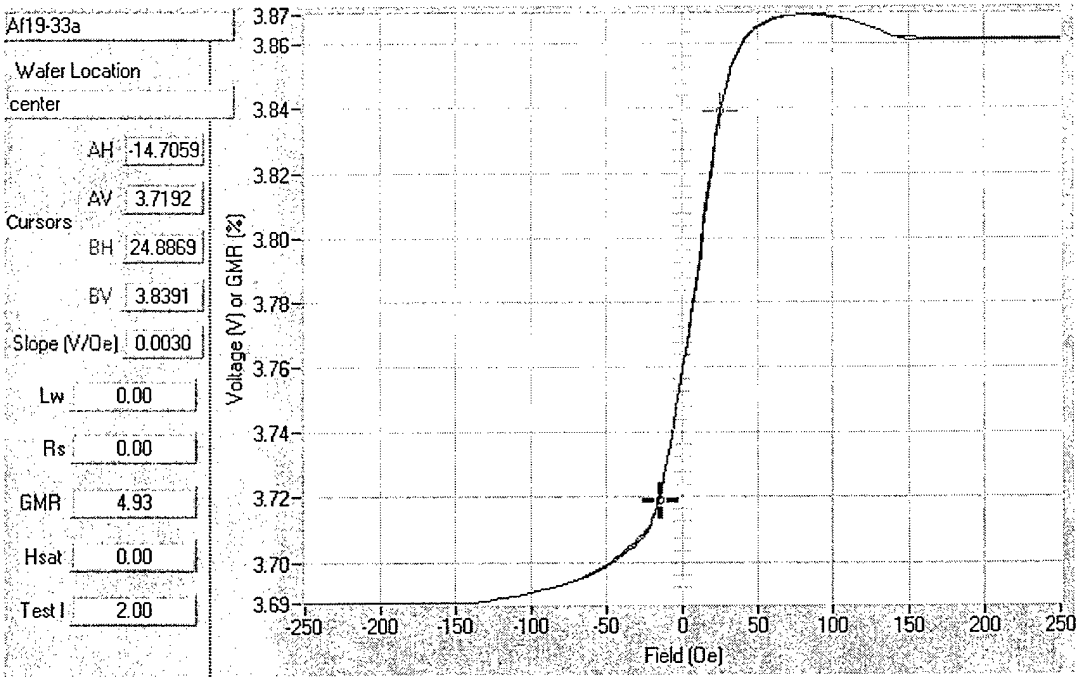

Figure 12. Two terminal resistance data from the new sandwich free layer GMR device.

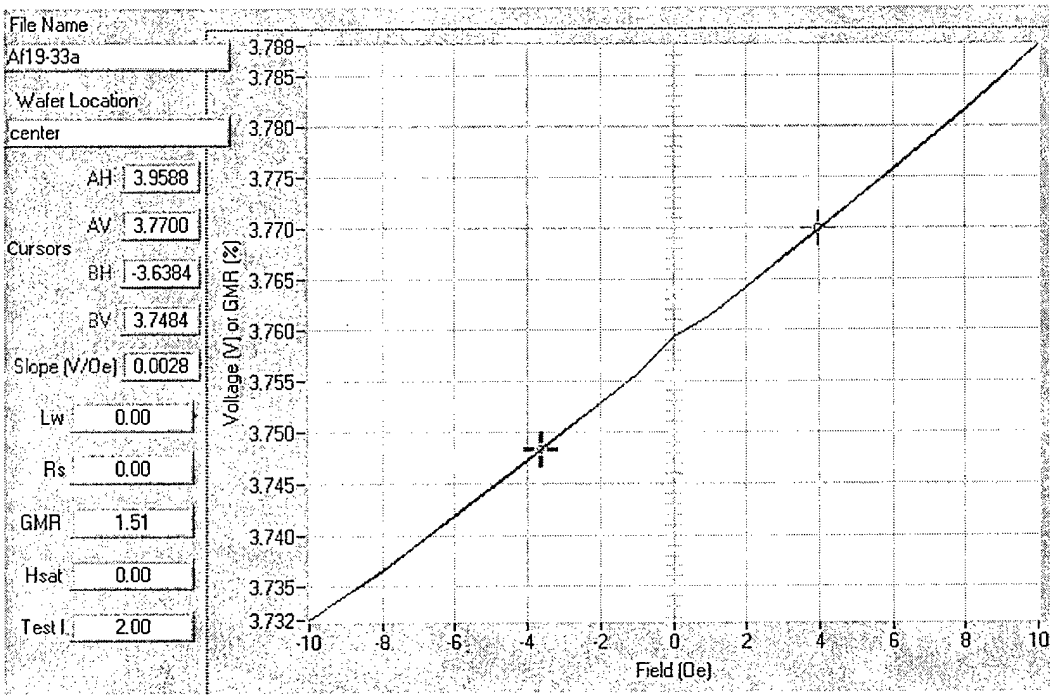

Figure 13. Low field sweep of the same GMR device as in Fig. 11. The small blip at zero field is an instrumentation artifact.

3. Low Power Sensor Results: transfer curve and noise evaluation

Three wafers worth of low power SDT sensors were packaged in SOIC-8 packages. This yielded about 3000 parts. About 30 of these parts have been hand-tested. An automatic test routine is being prepared to handle the parts in NVE's automated magnetic sensor test system. There are two types of parts whose resistance values are about 50 kΩ and 300 kΩ. The transfer function from one of the 300 kΩ parts is shown below in Figure 1.

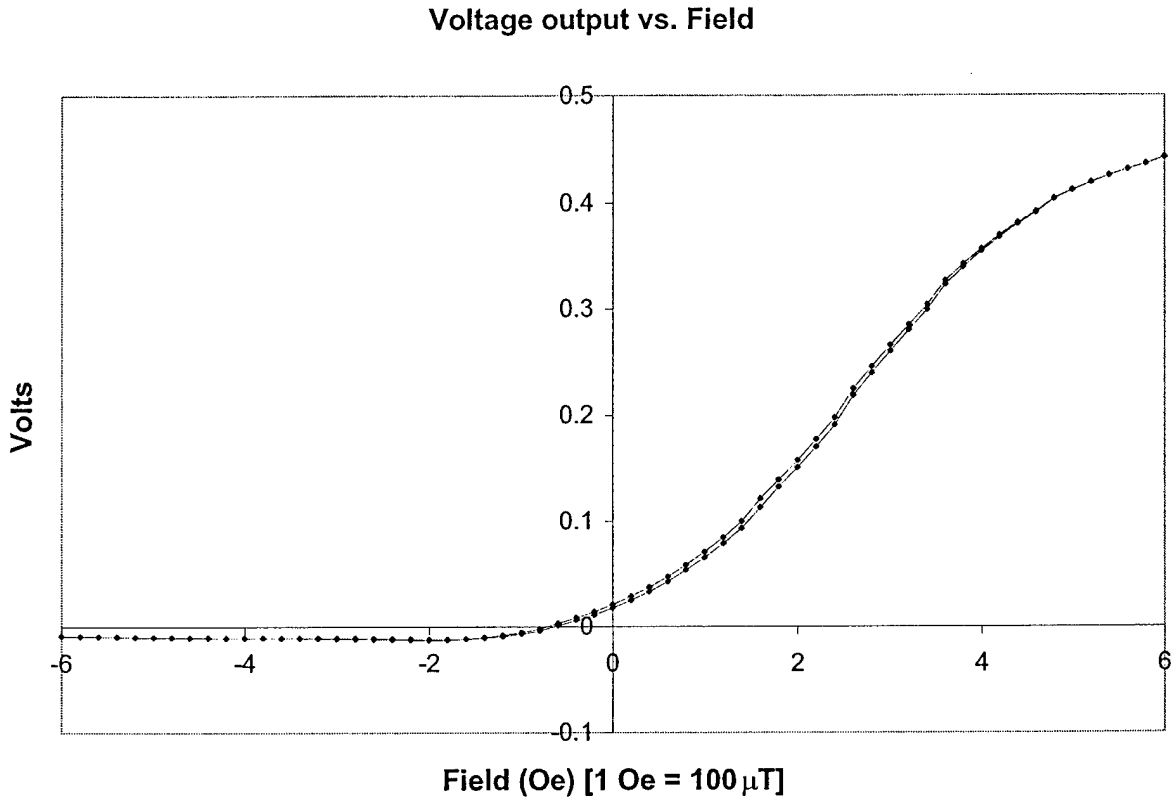

Figure 1. Voltage output vs. Field for an SDT magnetic field sensor. This output is from a resistance bridge whose legs are each nominally about 300 kΩ . The bridge is being supplied with a 5 Volt excitation. Thus, the output range of roughly 500 mV represents about 10% of the total excitation voltage.

This sensor output is not completely ideal. The ultimate objective is to get the transfer curve centered at the origin. There is still some hysteresis, the saturation field is higher than desired (+/- 2 Oe), and the total voltage change is relatively low (should be about 25% of bridge excitation rather than 10%. Nonetheless, the output is usable NOW as an unbiased field sensor.

The total power consumed by the transducer at 5 Volts bridge excitation is V^2 / R = (25 V^2 / 300,000 Ω) = 83 μW. This value is well below the value as stated in the SBIR

solicitation (1 mW / axis). However, the power for an amplifier is not included here. See section 4 for a power analysis that includes a low noise amplifier.

The field equivalent noise for the sensor is shown in Figure 2 below. The data were taken in a zero-gauss can having four concentric mu-metal shields. The noise of sensors is expected to vary considerably from one to another. No effort has been made yet to find the "good" sensors out of the batch of 3000, so it would not be surprising to see some sensors with up to ten times better noise than this one. There is, of course, no guarantee...

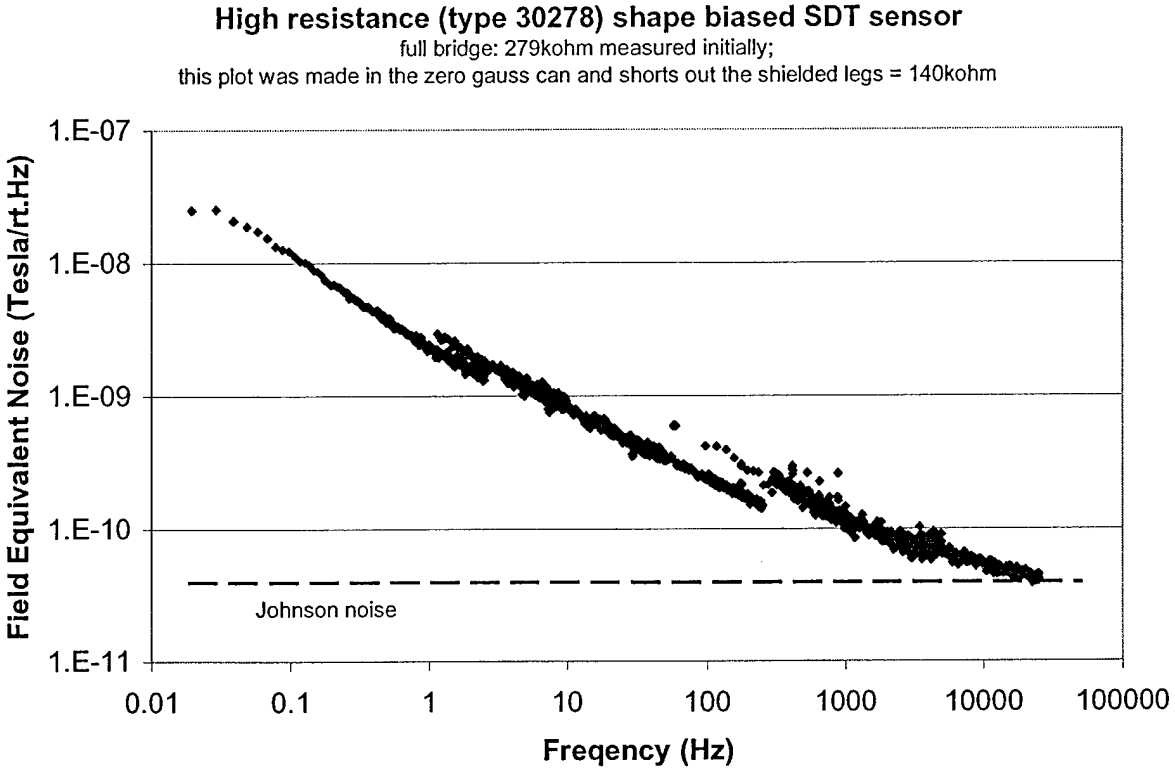

Figure 2. Field equivalent noise vs. Frequency. These data are calculated by measuring the voltage noise (Volts / rt. Hz) and dividing by the sensitivity (the slope of Figure 1, having units of Volts / Tesla). The gaps in the noise spectrum are due to mismatches in the various spectrum analyzer frequency ranges. The Johnson noise limit is shown as a reference point. Higher frequency values for noise should fall on this line.

This demonstrated noise falls short of the sensitivity goal stated in the SBIR solicitation by about one decade. Given the many areas where there are known shortcomings with this particular sensor, there is good reason to think another decade of sensitivity can be had with this type of sensor.

The fabrication and testing work presented here has been achieved with support from two additional research projects. An AF SBIR for fuzing development (POC Amy

Hermann, Eglin AFB) has been responsible for some of the fabrication work, and an Army SBIR for Unattended Ground Sensors (POC Alan Edelstein, ARL Adelphi) has supported some of the testing.

4. Power analysis

In order for the SDT low power sensors to be used in a system, it is expected that at least one stage of amplification is required. This may be only for buffering. Nonetheless, citing the power requirements of a resistance bridge transducer without also adding a provision for a low noise amplifier is not disclosing the whole picture. Therefore, a study was undertaken to examine the power requirements of a [transducer + amplifier] combination. The resulting paper was presented at the 2002 SPIE AeroSense conference, and is included below as it was submitted for publication. The summary of the result is that to achieve a noise floor of 5 pT / rt. Hz, a [magnetoresistive bridge + amplifier] combination will require about 1 mW for a single sensor axis.

Low-power 3-axis magnetometers using spin dependent tunneling for UGS and security applications

Mark Tondra, Albrecht Jander, Catherine Nordman; NVE Corp., 11409 Valley View Rd., Eden Prairie, MN 55344

ABSTRACT

Spin Dependent Tunneling (SDT) magnetic field sensors are under development as high performance magnetometers for Unattended Ground Sensing applications. These sensors have been successfully incorporated into a 3-axis magnetometer circuit for prototype level demonstrations with noise floors on the order of 1 nT / root Hz. @ 1 Hz. Future versions of these magnetometers will require lower power and lower noise floor than the existing prototype. This paper examines near term developments in the SDT magnetometer power requirements, considering the transducer + amplifier combination as the basic unit. An emphasis is placed on discussing the trade-offs between low power and high sensitivity. The impact of both SDT transducer impedance and amplifier power and noise are considered. Projections show that a 1 pT / rt. Hz @ 1 Hz noise floor is achievable in a transducer + amplifier unit consuming 1 to 10 mW. SDT sensors are being made in an effort to reach these goals. Special emphasis in this paper is on efforts to make an intrinsically low power transducer. Further discussion will explain some fundamentals of SDT sensor operation and how they impact ultimate expected magnetometer performance.

Keywords: Magnetometer, Spin Dependent Tunneling, Magnetic Tunnel Junctions, Magnetoresistance, Unattended Ground Sensors, Magnetic Field Sensor, Low Power, 3-Axis

1. INTRODUCTION

Magnetoresistive sensors, when used as magnetometers, have long offered an excellent combination of small size, low power, mass manufacturability, and low cost. These attributes make them particularly attractive for potential deployment in Unattended Ground Sensor (UGS) configurations. The same arguments hold for security applications, though the high volume production requirements may not be as dramatic. Their performance, however, is generally one notch lower than typical off the shelf fluxgate magnetometers.

The most common magnetoresistive magnetometers are based on the Anisotropic MagnetoResistance (AMR) effect. This effect has been known for over a century, and has been applied to many sensing applications ranging from magnetometers, to position sensors, to hard disk read heads. Two newer generations of magnetoresistive materials have been discovered and developed in the past ten to fifteen years. Giant Magnetoresistance (GMR) and Spin Dependent Tunneling (SDT) materials are similar to AMR in that they form intrinsically integrated thin film based devices. SDT devices have significant advantages over AMR devices in sensitivity. In fact, the magnetoresistance of a typical SDT device changes by 20 times that of an AMR device for the same range of field operation (40% vs. 2%). This means that, in practical magnetometer applications, the signal to noise could improve by about 20 times for the same range of operation. Based on these considerations, SDT sensors have the potential to operate at a noise floor approaching 1 pT / rt. Hz @ 1 Hz. Calculations to this effect (1) account for the thermal

noise and assume reasonable values of sensitivity. They do not account for 1/f noise, which has presented a difficult challenge for high performance operation at low frequency.
Ongoing efforts to realize this potential have resulted in usable SDT sensors. They have been incorporated into several kinds of magnetic detection systems, most relevant to the present topic being magnetometers. The most recent version of SDT magnetometer has full 3-axis capability. The three axes are each measured by individual 1-axis SDT sensors having mutually orthogonal orientations. A photograph of this magnetometer is shown in Fig. 1. These SDT sensors are described in detail in a previous SPIE proceedings (2). The sensor work describe in later sections of this paper differ from existing SDT sensors in the way they are put into their ideal operating condition. The standard version requires some 10 to 20 mA of current through an on-chip coil to generate a "perpendicular bias field" for the sensing film. The newer version, whose design and operation are described below, achieves linear magnetic operation through "shape biasing" rather than field biasing. Shape biasing is desirable because it does not require current (electrical power) to create it.
SDT sensors have the interesting property of having an extremely wide range of possible resistances. A typical sensor could be anywhere from 100Ω to 1GΩ depending on the thickness of the Al_2O_3 tunnel barrier that forms the resistance being measured. High impedances are attractive for their low power requirements. However, there is generally a tradeoff with noise floor vs. impedance. This paper investigates the utility of high impedance sensors, and discusses the practical aspects of amplifier selection and signal to noise as a function of power consumed in the SDT sensor + amplifier system.

For the sake of clarity, we define the transducer + amplifier system to include only amplification and not digitization. Most UGS systems are likely to have a single digitizer shared amongst all the clustered devices. The digitizer may or may not have an embedded amplifier. The sensor + amplifier system presented here would not require an in-A to D amp.

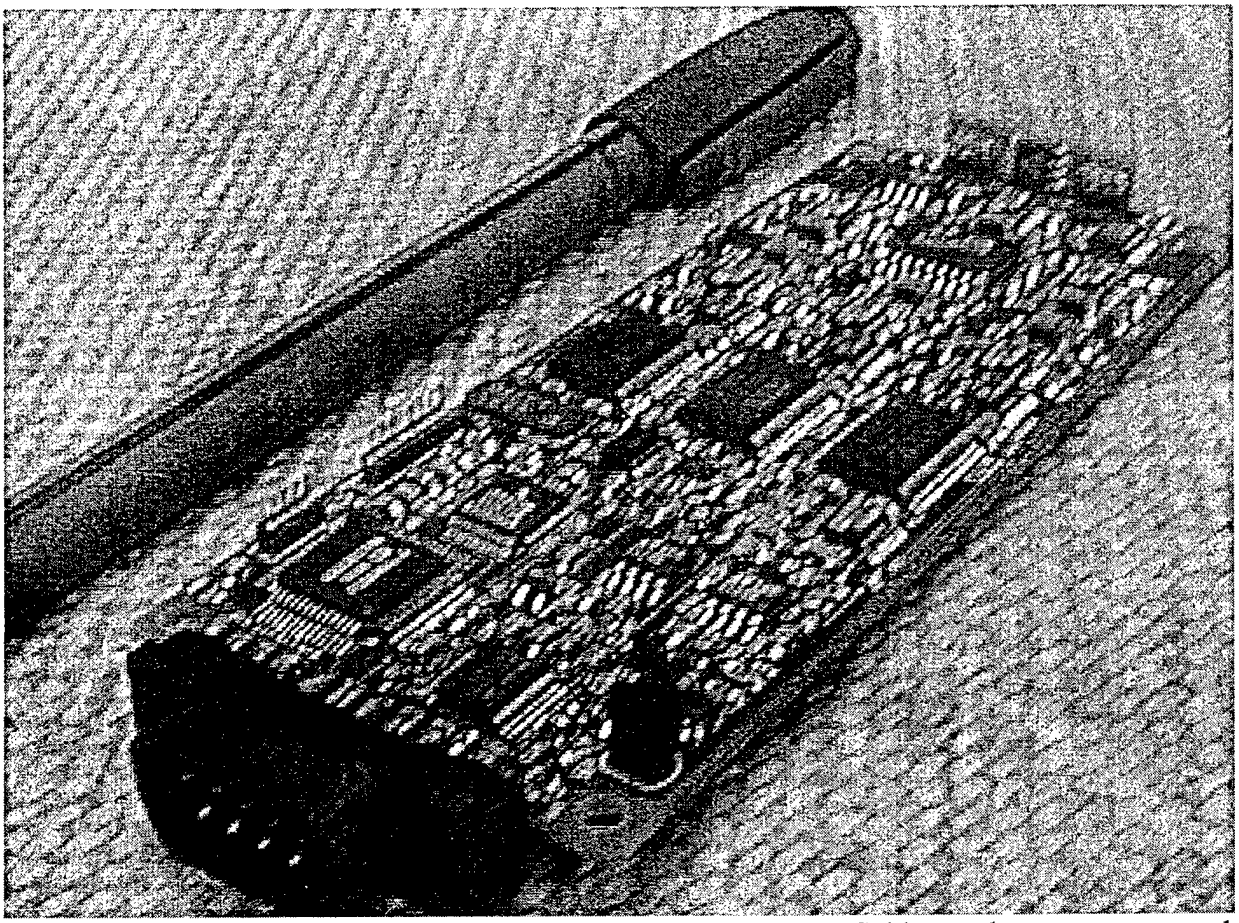

Figure 1. 3 Axis SDT magnetometer. The three single-axis SDT field transducers are mounted on the upper right end of the board, and take up relatively little area compared to the other attendant electronics for signal digitization, digital communication, and data processing.

2. BASIC POWER – RESOLUTION CONSIDERATIONS

1. Noise sources

The achievable sensitivity of magnetoresistive sensors is limited by several sources of noise. These include Johnson noise, shot noise, amplifier noise, 1/f noise and magnetic domain noise. Here we will consider only the first three, which are required by the laws of thermodynamics. The character and magnitude of 1/f noise and magnetic domain noise vary widely from device to device and it is difficult to present a generalized analysis. Furthermore, one can reasonably expect that these excess noise sources will be continually reduced due to ongoing sensor development efforts.

Johnson noise is the noise produced by the thermal agitation of carriers in a resistor. It power spectrum is "white" over a wide range and its RMS amplitude depends only on the absolute temperature T and the resistance R

$$V_{N,Johnson} = \sqrt{4k_B T\, R} \quad [V/\sqrt{Hz}],$$

where k_b is Boltzmann's constant (1.38×10^{-23} Joule/K).

Shot noise is due the fact that the device current consists of discrete events of electrons tunneling through the barrier. The variation in current due to the statistical nature of individual tunneling events is also "white" and increases with device current, I, as:

$$I_{N,Shot} = \sqrt{2qI} \quad [A/\sqrt{Hz}],$$

where q is the electron charge (1.6×10^{-19} coul). For a given bridge resistance, $V=IR$ and the RMS shot noise can be expressed as a noise voltage:

$$V_{N,Shot} = \sqrt{2qV_{bridge}R} \quad [V/\sqrt{Hz}].$$

These noise sources are intrinsic to the magnetic sensor. Additional noise is invariably introduced by the sense electronics. The noise introduced by an electronic amplifier is expressed as an equivalent input voltage noise that depends on the design of the amplifier. The chart in Figure 2 shows the input voltage noise and power supply current of a large selection of commercially available amplifiers. It is clear that there is a tradeoff between noise and power consumption. The solid line on the plot indicates an approximate lower bound on the available amplifier characteristics. The equation for this line is

$$V_{N,amp} > \sqrt{\frac{0.05\ nV^2\ mA}{I_{\text{supply}}\ Hz}} \quad [V/\sqrt{Hz}].$$

The total noise is then computed from the sum of the squares of the independent noise sources. This noise can be expressed as an equivalent field noise given magnetoresistive sensitivity, S.

$$B_{N,total} = \frac{1}{S}\sqrt{V_{N,Johnson}^2 + V_{N,Shot}^2 + V_{N,amp}^2} \quad [T/\sqrt{Hz}]$$

Here S expresses the slope of the transducer transfer function of the SDT sensor in units of Volts / Tesla.

2. Power constrained resolution

Given the above relationships between bridge resistance, supply current and noise, we can estimate the finest resolution achievable under the constraints of a power budget. The power consumed in the sensor bridge is

$$P_{bridge} = V_{\text{supply}}^2 / R$$

while the power consumed by the amplifier is a minimum of

$$P_{amplifier} = V_{\text{supply}} I_{\text{sup ply}}$$

If we assume a magnetoresistive sensitivity, S, of 1% (full scale voltage) / microTesla then we can plot, as in Figure 3, the achievable field resolution and total power consumption as a function of the bridge resistance and amplifier noise. Though the analysis was performed for SDT magnetic field transducers, it can be applied rather generally to any bridge + amplifier combination. The results shown would scale directly with sensitivity S, and the power supply voltage V. The resolution values shown are "flat" in frequency since the assumed noise sources are as well. Clearly, the presence of 1/f noise in real devices will add noise at the low frequencies. And since the assumed sensitivity of 1% / microTesla is fairly optimistic, the results in Fig. 3 are best thought of as a lower bound on the noise floor of an SDT transducer +

amplifier system operating at 5 Volts. The frequency range of validity for this calculation depends on the gain-bandwidth characteristics of a given amplifier. It is reasonable to expect that the cited amplifiers can perform most desired functions up to 100 kHz or so.

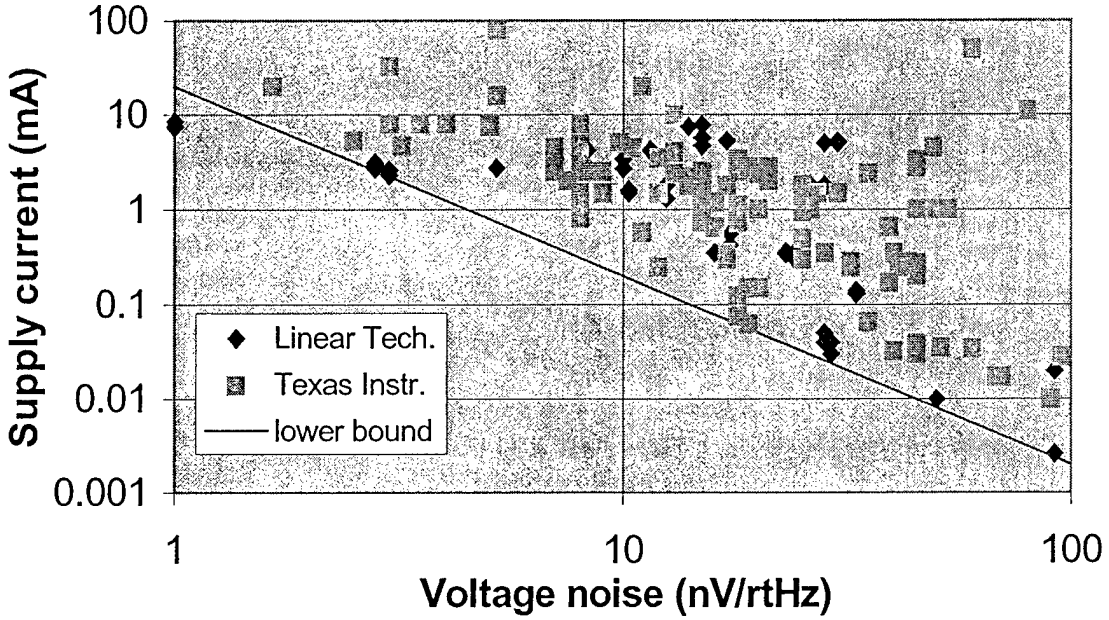

Figure 2. Power supply current vs. input referred noise voltage of commercially available operational amplifiers.

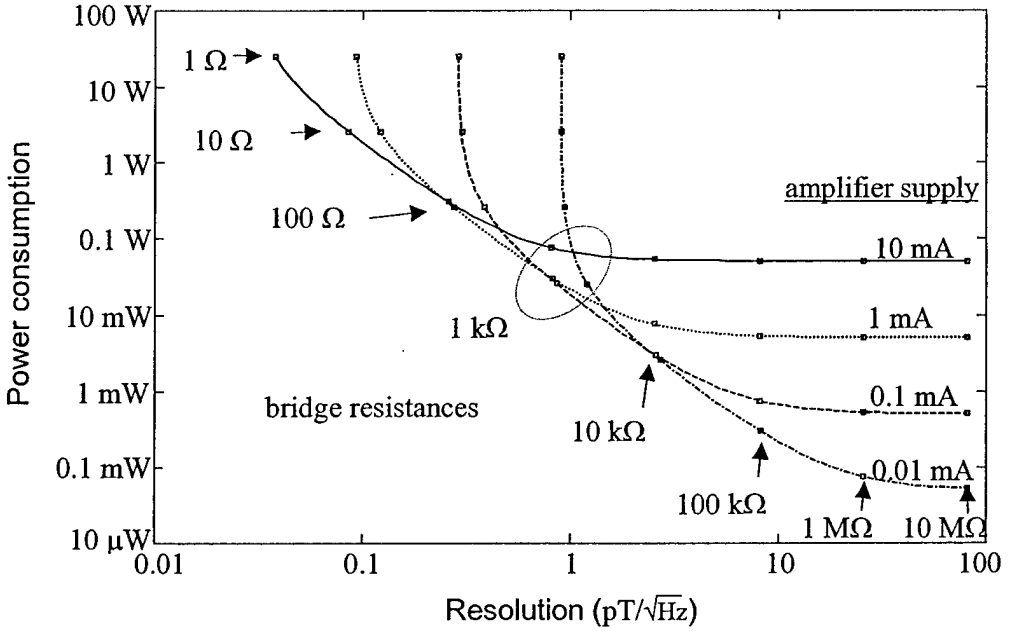

Figure 3. Power consumption versus resolution for magnetoresistive sensor systems operating at 5 volt supply. The curves are for different amplifiers while points along the curves represent specific bridge resistances. At high bridge resistance, the bridge noise dominates the resolution while the choice of amplifier determines the power consumption. At low bridge resistance, the amplifier noise dominates the resolution and the bridge resistance determines the power consumption.

3. SDT TRANSDUCER MAGNETIC OPERATION

As mentioned in the Introduction and described in detail elsewhere (2), recent versions of SDT sensors consume significant power (~100 mW) to generate the magnetic field bias needed for linear sensing. This power in not an intrinsic feature of SDT sensors, but rather, the result of *one method* to create a linear sensing condition. The underlying magnetics problem is to cause the magnetization of the sensing or "free" layer of the SDT sensor to rotate smoothly through a full 180 degrees as the external field along the sense axis changes from negative to positive. This rotation and the resulting sensor voltage output is suggested in the schematic shown in Fig. 4.

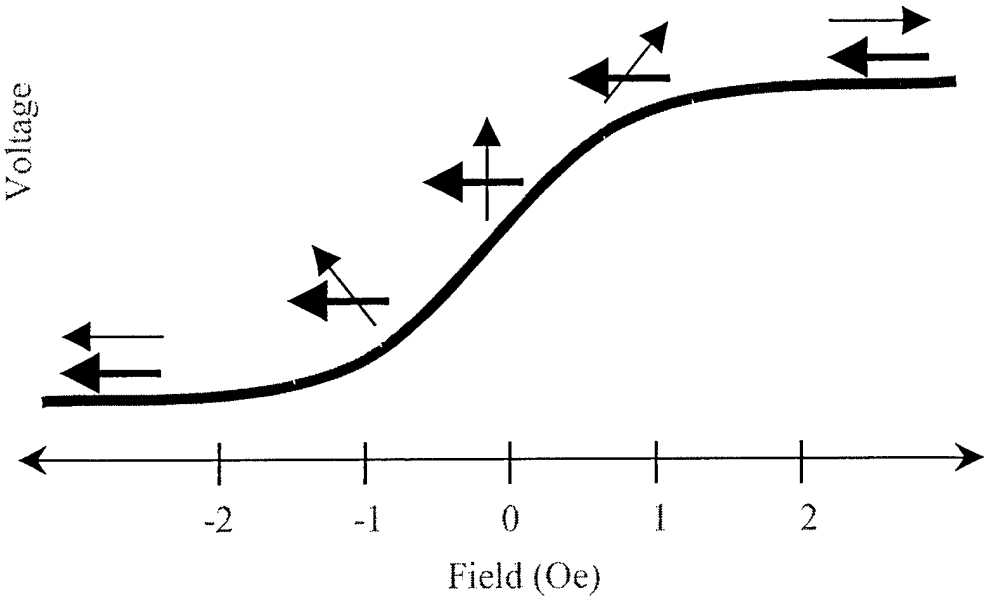

Figure 4. Voltage output vs. Field of a linear SDT sensor with appropriate magnetic biasing. The thicker arrow indicates the orientation of the magnetically "pinned" layer. The thinner arrow represents the orientation of the "free" layer. Note that the middle resistance value, observed at zero field, occurs when the two magnetic layers are perpendicular. The minimum output occurs for the parallel orientation while the maximum output occurs for the antiparallel orientation.

An alternative method for creating the ideal perpendicular magnetic bias condition is to use "shape anisotropy" to force the free layer magnetization to lie along the desired orientation in zero applied field. Shape anisotropy basically means that the magnetization of dimensionally constrained ferromagnetic objects prefers to be along the longest dimension. By making a thin film into a long and narrow "stripe" one creates a preferred orientation along the stripe. If the pinned layer is made to lie across the stripe, then the perpendicular configuration is achieved

without any additional applied field. It is precisely this technique that is being applied to SDT sensors here. Such techniques have been described for tunnel junction (3) and GMR spin valve (4,5) devices before. However, they have focussed on read head or MRAM applications. This paper discusses the utility of shape biasing in linear field sensors.

4. SDT TRANSDUCER FABRICATION

In order to achieve shape biasing in SDT devices, a special set of photolithography masks were designed and purchased. The patterns in these masks were designed to create tunnel junctions with large aspect ratios, and the long direction of the narrow junctions is oriented perpendicular to the sensing direction. Three different designs were put on the same set of photolithography masks. All three designs had the same aspect ratio (15:1) for the sensing film. The widths of the sensing layers for these three designs are 2 μm, 6 μm, and 10 μm. Patterning and annealing steps must be performed in the correct sequence in order to achieve optimal results.

The layers in the SDT stack are NiFeCo 125 / Al_2O_3 15 / FeCo 50 / Ru 9 / FeCo 50 / CrPtMn 300 (in Angstroms). The free layer (bottom) is deposited in a 20 Gauss field such that its easy axis is perpendicular to the sensing direction. The pinned layer is also oriented in this direction initially, but is rotated to be parallel to the sensing direction in subsequent processing steps. A post-deposition anneal is performed perpendicular to the sensing direction in order to enhance the stability of the free layer easy axis and reduce dispersion.

The narrowest of the three junction designs have top electrodes whose long edges are coincident with the edges of the bottom layer. The mask patterns for the top and bottom layers actually overlapped in a "plus sign" shape. They are formed by first etching the top electrode, then etching the second by cutting deeply enough to remove both top and bottom layer material. Because the second etch cuts fully through both layers, the the resulting junctions are not "plus" shaped. Rather, the bottom electrode is a long and narrow rectangle upon which two top junctions sit, which are also long and narrow rectangles. The sides of the tops are flush with the sides of the bottom. Two junctions are connected in series through a common bottom layer. This arrangement is shown schematically in Figs. 5 and 6. This narrow pattern results in a bottom electrode being 2 μm x 30 μm and top layers being 2 μm x 12 μm. The wider two junction designs have top electrode edges inset from the bottom layer by 1 to 2 μm (not shown here). The two-top-one-bottom arrangement permits higher density and makes subsequent processing of Al interconnection layers easier.

Etching is performed using a hard mask (silicon nitride) patterned with a reactive ion etcher (RIE). Once the hard mask is formed, a Commonwealth ion mill is used to etch the top electrodes. The ion mill etch is timed to on or just above the tunnel barrier layer. A wet etch is used to clean up any residual top layer material. A similar procedure is used to etch the bottom layer. However, the depth tolerance is not so critical. The mill is set to over-etch by several hundred Å.

Once the junctions are patterned, a second anneal is performed with a field applied perpendicular to the sensing direction to enhance the properties of the sensing layer. A final anneal is performed with the field parallel to the sense direction. This last anneal reorients the pinning direction and results in the desired orthogonal sensing configuration. The present process calls

for one hour at 250 ^{O}C in 2400 Oe for the first and second anneals. These anneals create an acceptable result. However, considerable improvement should be possible with some refinement of the process and better starting material. The annealing process challenge is to get the pinning layer reoriented without significantly degrading the magnetic properties of the free sensing layer or the magnetoresistive properties of the tunnel barriers.

The magnetoresistive response of tunnel junctions patterned in this way is shown below in Figs. 7A and 7B. These data are from junctions with 10 μm x 150 μm bottom electrodes and 6 μm x 70 μm top electrodes (area = 420 μm^2). The resistance of each junction is approximately 1 kOhm, and the resistance area product (RAP) = 420 kOhm - μm^2. The magnetoresistance is considerably lower than ideal (6% vs. ~40%). (The NVE record to date for similar junction types is 44%, and >30% is common). This is an indication of the barrier quality of this wafer and not of the overall magnetic sensing configuration. One would expect to be able to craft the same magnetic behavior in a 40% MR device.

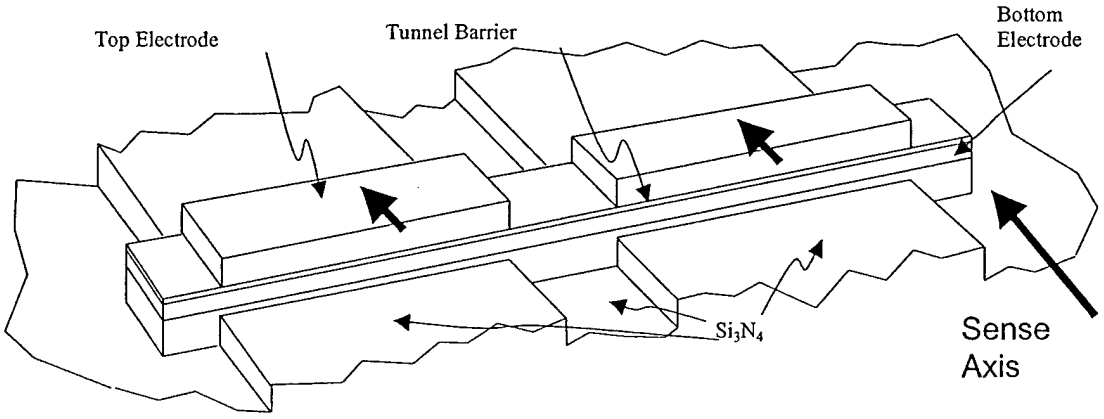

Figure 5: A schematic cross section of the shape biased SDT elements. Shown here is a pair of SDT elements sharing a common bottom sensing film. This is drawn to suggest the surface topology after the "plus" shaped mask pattern process. The material directly beneath the bottom electrode is Si_3N_4. The thick arrows in the top regions indicate the orientation of the magnetization of the pinned layers. The easy axis of the free layer is along the long direction, perpendicular to the magnetization of the pinned layers.

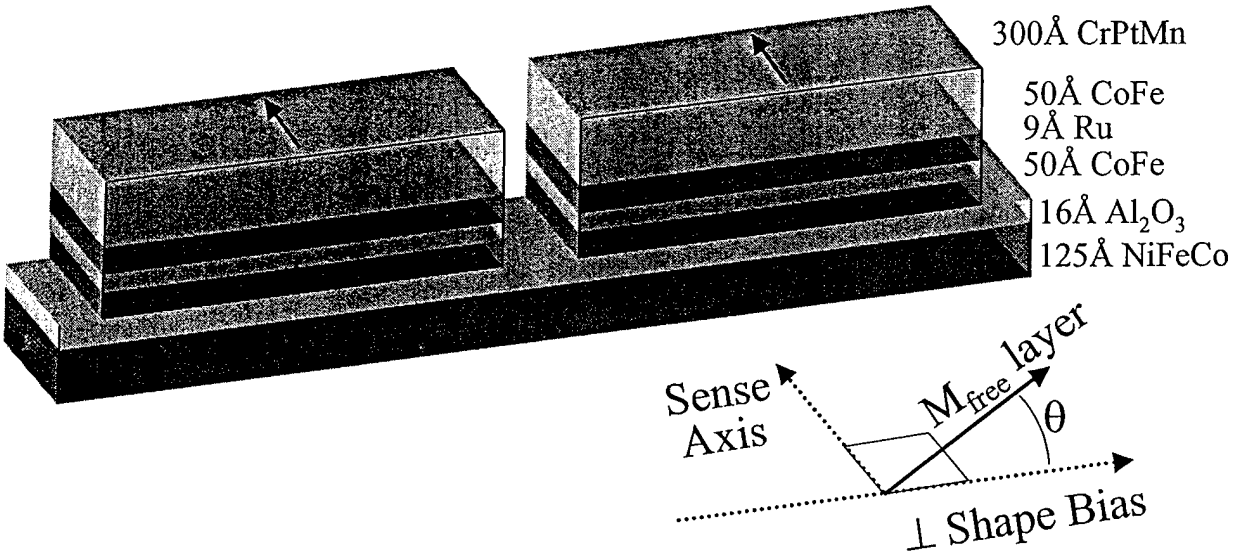

Figure 6. The shape biased SDT junction pair with the detailed magnetic layer structure indicated.

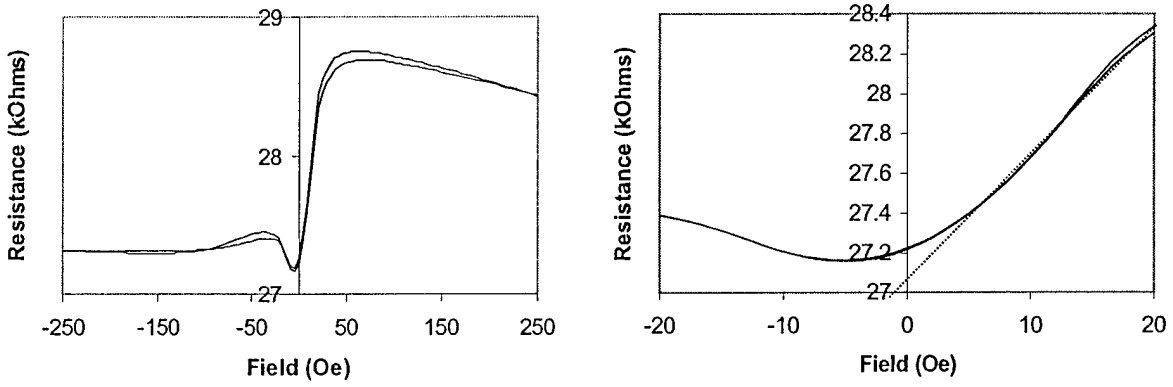

Figure 7A. A wide field sweep of the resistance of a shape biased tunnel junction bridge. It is a Type 3 bridge (see table 1 below) having 20 of the 6 μm x 70 μm junctions in each bridge leg. Figure 7B. The small field range resistance vs. field response for the same device as in Fig. 7A. The "sweet spot" on this sensor is at about 10 Oe, where there is no hysteresis and large slope (suggested by the dotted line).

5. DISCUSSION AND CONCLUSIONS

The power required to run full SDT sensor bridges depends on a number of issues. The bridge power is simply V^2 / R, where V is the voltage and R is the resistance. V is typically fixed at a value like 3.3 volts. R, however, depends on the bridge configuration and the RAP.

R = (# junctions per leg) x (resistance / junction) = (# per leg) x (RAP / junction area) (1)

The three bridge designs all have the same total area for tunnel junctions, approximately a region 60 μm x 600 μm, in the gap between two flux concentrators. A larger number of small tunnel junctions or a smaller number of large tunnel junctions can fit into this same space. Table 1 summarizes the properties of the three bridge designs in terms of physical dimensions, numbers of junctions, junction resistance, and power consumption assuming a 3.3V supply.

The operating voltage is not likely to change much, and is typically dictated by circuit considerations. However, it is relatively easy to vary the RAP over many orders of magnitude. Furthermore, a larger RAP is easier to make than a smaller RAP. This is because it is relatively easier to make high quality junctions (no voids or pinholes) as the barrier gets thicker. Much research effort has been devoted to *reducing* RAP for devices like read heads and MRAM because they need to operate at 1 GHz and have a correspondingly small resistance-capacitance (RC) time constant. For low frequency field sensors, no such speed requirements exist. Thus we suggest that a 1 GΩ-μm^2 RAP might well be appropriate for the sensor designs described in this paper. This would reduce the power figures in Table 1 by a factor of 1000, and result in a 1 nWatt SDT sensor (amplification not included) in the case of Design #3.

The most important result presented here is that, based on calculations accounting for Johnson, shot, and amplifier noise, a noise floor on the order of a few pT / rt. Hz @ 1 Hz is achievable for an SDT sensor + amplifier unit consuming 1 mW. Such a device has performance on par with the best fluxgate magnetometers, but consumes orders of magnitude less power and space. From

a sensor development standpoint, this is possible only if the cross-axis biasing is used to eliminate the need for current-based field biasing of the sensor. It should be noted that surplus 1/f noise has been observed in all SDT sensors made to date. This 1/f noise, however, is not a physically required aspect of the SDT sensors, and further development of the SDT technology will likely reduce the 1/f noise in finished sensors.

Of additional interest is that as the bridge resistance increases by orders of magnitude, the SDT Johnson noise dominates the SDT + amplifier system noise. If one were to be satisfied with 1 nT / rt. Hz @ 1 Hz, it could be achieved in a sensor + amp system consuming about 50 microWatts. Since the amplifiers studied for this paper are best suited for bridges in the 1 to 100,000 Ω range, additional investigation is required to make good estimates of the power required for *practical* 1 GΩ devices.

Bottom Electrode (μm x μm)	Top Electrode (μm x μm)	Junctions per Leg	Area (μm^2)	Resistance @ 1MΩ-μm^2 (kΩ)	Power @ 3.3Volts (μW)
2 x 30	2 x 10	216	20	10,800	1
6 x 90	4 x 40	60	160	250	40
10 x 150	6 x 70	20	420	29	350

Table 1: Dimensions for the three bridge designs. The resistance area product (5th column) is the most widely controllable parameter in SDT fabrication.

6. REFERENCES

1. M. Tondra, J.M. Daughton, D. Wang, R. Beech, A. Fink, and J. Taylor, "Picotesla field sensor design using spin-dependent tunneling devices," J. Appl. Phys., vol. 83, pp. 6688-6690 (1998).
2. M. Tondra, Unattended Ground Sensors and Technologies III, E. Carapezza, editor. Proceedings of the SPIE, Vol. 4393 (2001).
3. B. Schrag, A. Anguelouch, G. Xiao, P. Trouilloud, T. Lu, W. Gallagher, and S.S.P. Parkin, J. Appl. Phys., 87, 4682 (2000).
4. S. Mao, J. Giusti, N. Amin, J. Van Ek, and E. Murdock, J. Appl. Phys., 85, 6112 (1999).
5. K. Moon, R. Fontana, and S.S.P. Parkin, J.Appl. Phys., 74, 3690 (1999).

5. CUFG Application Possibilities

The "Clutter-Limited Detection" solicitation lists several desired performance items. Magnetoresistive sensors in general, and low power SDT sensors in particular, can potentially meet all of the requirements. In the case of SDT sensors, the only requirements that pose a serious technical challenge are power and sensitivity. These are presented below as they appeared in the program solicitation:

- *(B) Low power: less than milliwatt of average power per receiver;*
- *(D) High sensitivity: for B field, noise equivalent performance less than 5 picoTesla/root Hz in the 10 Hz to 300 Hz frequency range, noise equivalent performance less than 0.5 picoTesla/root Hz in the 300 Hz to 2000 Hz frequency range; noise equivalent performance of electric-field sensors should be below the clutter background.*

With the results obtained in this Phase I SBIR project, the power requirement is no longer an issue. The noise requirement is well within the theoretical capabilities of the SDT technology, though continued development of the sensor materials will be required.

Self-Orienting concept One challenging aspect of the CUFG application is that the detectors need to be remotely deployable. They need a way to determine their relative positions and orientations after they have been fielded. A magnetic way to do this is with a magnetic field communications system. Such a system is being developed by Aura Communications (Wilmington, Mass.) for very short range communications. The system specs call for 5 mW to communicate magnetically with nodes about 1 meter away. Their system uses coils as pickups, but could just as easily use SDT sensors. The key point is that the magnetic orienting system generates magnetic fields with a 3-dimensional vector quality. The magnitude of the field goes as 1/distance^3, so the magnitude is an indication of the distance from source to detector.

In a CUFG application having about 10 detector nodes, 3 of the 10 could have field sources in addition to a 3-axis SDT detector. The sources would be programmed to transpond for a few seconds at a somewhat higher power level (say 1 Watt) to achieve a range of 10 to 100 meters. The 10 detector nodes would monitor this activity, and the system would determine each node's location and orientation based on the response to these three field sources. Once the setup phase is complete, the coils would be off, and the detectors would operate in low-power mode.

Appendix A. Phase I Work Plan (as in proposal)

Tasks will be carried out on the following schedule:

		Month							
	Task	1	2	3	4	5	6	7	8
1	Program plan								
2	Comparative Technology Study								
3	Fabricate Low Power SDT Sensors								
4	Demonstrate sub mW SDT Sensor								
5	Evaluate Calibration, Orientation, and Detection Concepts								
6	Project performance of Phase II prototype								
7	Final report								

The project performance period ends on June 28, 2002. The final acceptance of the final report must take place within three months of this date.

Appendix B. Budget

The total budget was for $98k over an 8 month period. Nearly all of this amount has been spent. As of 7-24-02, there is about $3000 left, which should be sufficient to cover the preparation of this final report and other program-ending tasks.

Appendix C. Comparative Technology Study (from 1st quarter report)

Work to date has focused on learning about varieties of magnetometers including AMR, fluxgate, and coils. Additional work is required in the area of potential electric field sensors, and learning about the expected signatures to be measured. Magnetoresistive devices (especially tunnel junctions) are reviewed here.

Best Integrated Magnetoresistive Sensor Material For small size, low cost, and ease of integration, nothing beats integrated thin film magnetoresistive sensors. Within the class of magnetoresistive sensors, SDT devices have a major advantage in sensitivity over other varieties.

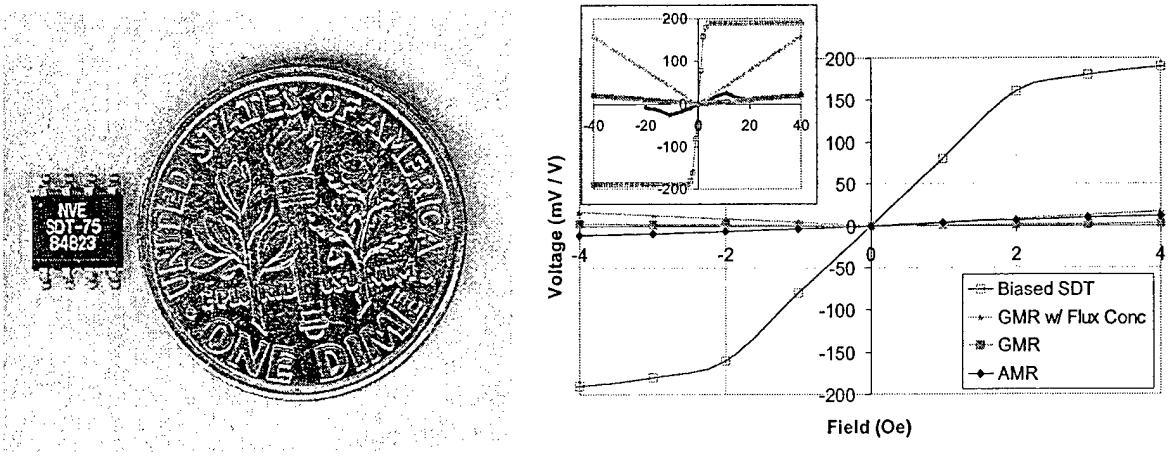

Figure 1: On the left is a picture of an SDT sensor next to a dime. On the right is a comparison of the output of three types of magnetoresistive sensors. The data is not from actual sensors but is representative of actual results and specifications. The SDT sensor has a flux concentrator, as does the upper GMR curve.

Due to their overwhelming benefits of high sensitivity and high resistance (low power), SDT devices merit a significant development effort. Specifications for prototype SDT sensors are shown here:

	State of the Art	
Noise floor at 1 Hz	289 pT / rt. Hz	Best result
Noise floor (hi freq.)	7 pT / rt. Hz	Best result
Magnetoresistance	44%	Best result
Dynamic range	+/- 200 μT (2 Gauss)	Typical
Hysteresis	0.08 Oe on full sweep	Typical
Linearity	feedback required	
Bridge power	1 mW (10kΩ @ 2.5V)	Typical
Orthogonal Bias power	200 mW (500Ω @ 10V)	Typical
Die size	1775 μm X 2210 μm	
Package	SOIC-8 (5mm x 6mm)	
Cost (low volume)	~$6	
Cost (high volume)	~$1	
Reproducibility	over 10,000 made	not production qualified

Noise floor One critical limitation of the present SDT sensors is their noise level at low frequency. There is a considerable 1/f noise component in the voltage vs. frequency spectrum. When the sensor is operated at its maximum voltage level, the corner frequency is about 10 kHz. Thus, the noise (in units of field / root Hz) at 1 Hz is two orders of magnitude higher than the intrinsic Johnson noise limit. The 1/f noise is "excess" in that there is no apparent thermodynamic requirement that it exist (in contrast to the Johnson noise). The best explanation for this 1/f noise is defects in the tunnel junction and its interfaces. Thus, one obvious path towards reduced effective field noise is to increase the barrier quality. Improvements in SDT quality have driven an impressive rate of improvement to date (shown in the figure below). NVE estimates that

another two to three orders of magnitude improvement in sensor performance at low frequency is possible in the next few years.

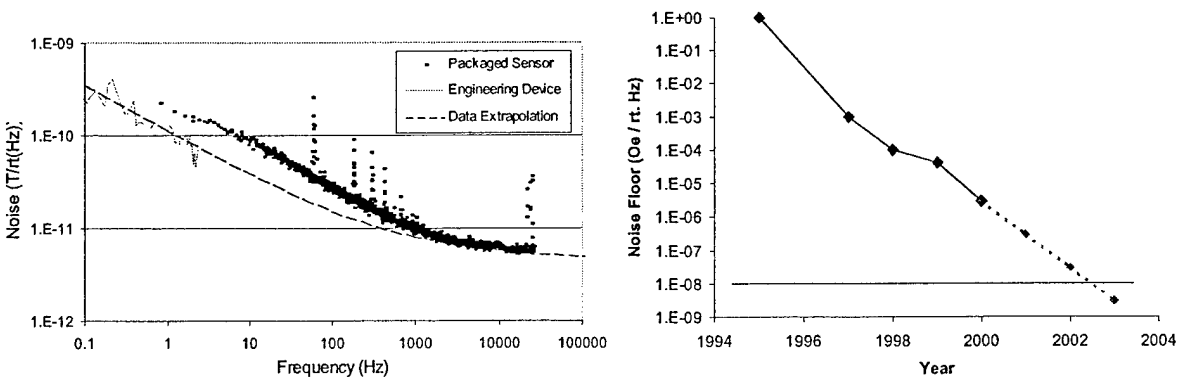

Figure 2: Effective field noise vs. frequency is plotted on the left. Effective field noise is calculated by dividing the voltage noise [Volts / root Hz] by the sensitivity [Volts / Tesla]. Effective field noise floor at 1 Hz vs. calendar year is plotted on the right. These points represent the best results from a given year. The solid horizontal line represents 1 pTesla / root Hz. 1 pTesla = 1 x 10^{-8} Oersted.